

THRUSTING OF THE HINDU KUSH OVER THE
SOUTHEASTERN TADJIK BASIN, AFGHANISTAN:
EVIDENCE FROM TWO LARGE EARTHQUAKES

Geoffrey Abers and Carol Bryan

Department of Earth, Atmospheric and
Planetary Sciences, Massachusetts
Institute of Technology, Cambridge

Steven Roecker

Department of Geology, Rensselaer
Polytechnic Institute, Troy, New York

Robert McCaffrey¹

Department of Earth, Atmospheric and
Planetary Sciences, Massachusetts
Institute of Technology, Cambridge

Abstract. We infer from the mechanisms and depths of two large earthquakes that the Hindu Kush is actively thrusting northwest over the Tadjik basin and that the basin is closing rather than being displaced to the west. Teleseismic body waves were used to determine focal mechanisms and depths for the two largest shallow earthquakes on the southern edge of the basin. The two earthquakes, on June 24, 1972 ($m_b=6.0$), and December 16, 1982 ($m_b=6.2$), have seismic moments of 2×10^{18} N-m and 6×10^{18} N-m, respectively. Focal mechanisms of both events indicate almost pure thrust faulting with nodal planes striking northeast-southwest. The inferred fault planes dip southeast, at 20° for the first event and 50° for the second. The P axes for both events are oblique to the direction of relative motion between India and Asia, suggesting that the Pamir is overthrusting the basin to the west. Depths for both earthquakes are between 20

and 25 km and place them well below the Tadjik basin sediments. The depths and steep fault planes suggest that these earthquakes represent a downdip extension within the basement of shallow folding and thrusting seen in the sediments northwest of the events. Thus convergence in Afghanistan between India and Eurasia is taken up along southeast dipping thrust faults north of the Hindu Kush as well as by northward subduction under the southern part of the range.

INTRODUCTION

Active deformation in central Asia is a consequence primarily of the collision of the Indian and Eurasian continents [Molnar and Tapponnier, 1975]. The modes of deformation include shortening along thrust faults (e.g., along the Himalayan front), lateral displacement along strike-slip faults (e.g., the Altyn Tagh and Kunlun faults), and extension along normal faults (e.g., in the high elevations of Tibet) [e.g., Molnar and Tapponnier 1975; Molnar and Deng, 1984]. Much recent investigation has concentrated on the mechanics governing these modes of deformation as well as their relative importance in accommodating continental collisions (particularly lithospheric thickening [e.g., England and Houseman, 1985] versus "extrusion tectonics" [e.g., Tapponnier et al., 1982]).

¹Also at Air Force Geophysical Laboratory, Hanscom Air Force Base, Bedford Massachusetts.

Copyright 1988
by the American Geophysical Union.

Paper number 7T0829.
0278-7407/88/007T-0829\$10.00

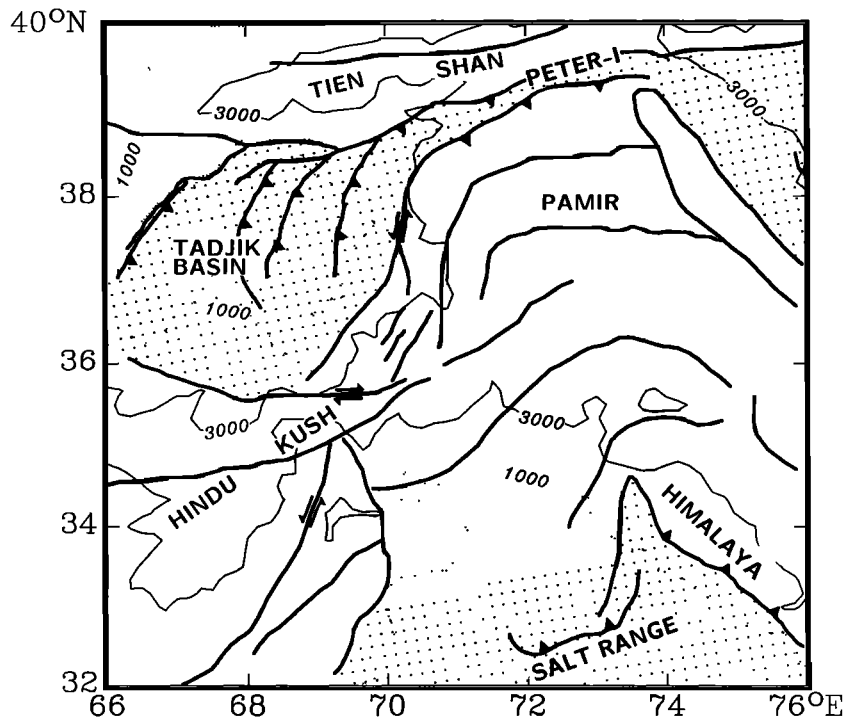


Fig. 1. Location map of Central Asia. Topography contours are in meters: Dotted line is the 1000-m contour and thin solid line is the 3000-m contour. Thick lines show major faults, labeled on Figure 2. Shaded areas show exposures of Mesozoic and Cenozoic sediments, modified from Stöcklin [1977].

This paper examines the active tectonics of the southeastern Tadjik basin, located near the westernmost boundary of the Indian plate in northeastern Afghanistan (Figures 1 and 2). The many active thrust faults north and east of this basin testify to the prevalence of crustal shortening in this area, while strike-slip motions along the Herat, Andarab, and Chaman faults predominate to the south and west. The basin is thus the locus of a transition between these two modes of deformation. We analyze the two largest recent earthquakes in the Tadjik basin in order to determine how regional convergence is being accommodated.

TECTONIC SETTING

The Tadjik basin is an area of relatively low relief flanked by major orogenic belts (the Hindu Kush, the Pamirs, and the Tien Shan; Figure 1). Up to 7 km of Miocene and younger molasse has been deposited in the eastern part of the basin, with the thickest accumulations

just west of the Darvaz-Karakul fault along the Pamir front [e.g., Zakharov et al., 1968; Leith and Alvarez, 1985]. The Neogene sediments overlie a 3 to 5 km thick shallow marine sequence [Peive et al., 1964], inferred to be deposited on a south facing passive continental margin in Mesozoic and early Tertiary time [Leith, 1982]. Since early Miocene time much of the northeastern Tadjik basin developed as a foreland fold-and-thrust belt that advanced to the northwest in front of the Pamir [e.g. Stöcklin, 1977; Leith, 1982]. A series of northwest verging sedimentary thrust sheets, presumably detached from the basement at a Jurassic evaporite sequence, has been identified on the north side of the basin [Gubin, 1960].

In the southeastern Tadjik basin, Tapponnier et al. [1981] observed large concentric folds and over 5 km of Plio-Pleistocene molasse tilted eastward toward the Pamirs. North to northeast trending anticlines have also been mapped in this part of the basin [Shareq, 1981]. Thus the southern Tadjik basin also probably has foreland fold belt structures.

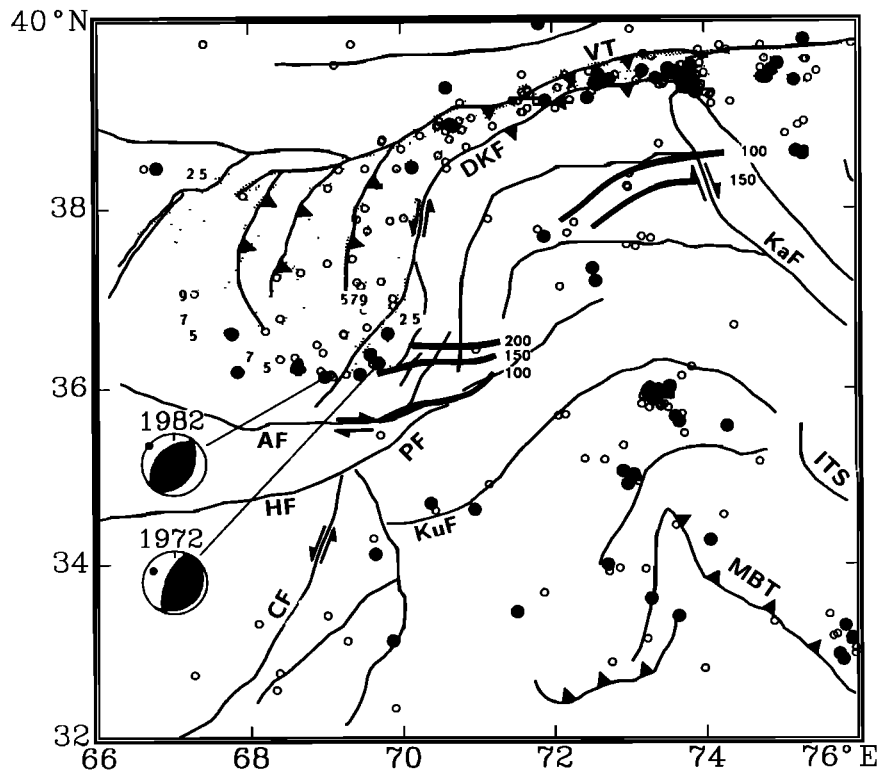


Fig. 2. Map of shallow earthquakes, major faults, and isopachs. Earthquake locations are from the ISC catalogue, 1971-1981, for earthquakes recorded by 15 or more stations and with depths ≥ 70 km, body wave magnitude ≥ 4.5 , and standard errors in latitude, longitude, or depth ≤ 25 km. Small open circles show epicenters of earthquakes with $4.5 \leq m_b < 5.0$ and large solid circles represent earthquakes with $m_b \geq 5.0$. Fault-plane solutions are lower-hemisphere projections for the earthquakes discussed here; the events are labeled by year of occurrence. Thick solid lines are contours of depth to the deep seismic zones, labeled in kilometers, modified from Billington et al. [1977]. Dotted lines show contours of depths (kilometers) to Paleozoic basement in the Tadjik basin and Peter I ranges, adapted from Marussi [1963]. Thin solid lines are major faults based on the compilations by Zakharov et al. [1968], Chatelain et al. [1980], and Shareq [1981]. Labeled faults are: VT, Vakhsh Thrust; DKF, Darvaz-Karakul Fault; KaF, Karakorum Fault; AF, Andarab Fault; HF, Herat Fault; CF, Chaman Fault; PF, Panjer Fault; KuF, Kunar Fault; ITS, Indus-Tsangpo Suture; and MBT, Main Boundary Thrust.

Earthquakes and Quaternary fault offsets associated with the surrounding orogenic belts testify to ongoing deformation at the borders of the basin. To the north, active thrusting has been reported along the Vakhsh thrust [e.g., Gubin, 1960] and in the southern Tien Shan [e.g., Nelson et al., 1987]. Strike-slip faulting has also been observed in the Paleozoic basement rock north of the Vakhsh thrust in the Garm region [e.g., Hatzfeld et al., 1986] and may extend further west [e.g., Trifonov, 1978;

Bazhenov and Burtman, 1986]. In the Peter I range, a belt of tightly folded Mesozoic sedimentary rocks contiguous with the relatively undeformed Tadjik basin, earthquakes reveal a complex juxtaposition of thrust and strike-slip faulting [e.g., Wesson et al., 1976; Hatzfeld et al., 1986]. East of the Tadjik basin, Kuchai and Trifonov [1977] infer 10- to 15-mm/a left-lateral motion on the north-northeast trending Darvaz-Karakul fault. To the south, geological evidence has been found for active right-lateral motion on the

east-west trending Andarab and possibly Herat faults [Wellman, 1966; Tapponnier et al., 1981]. Although many faults near the southern edge of the basin may be active strike-slip faults, there are few well-determined focal mechanisms for shallow earthquakes in this area. South of the Hindu Kush, earthquakes reveal high-angle thrusting at depths of 5-20 km [Baranowski et al., 1984; Jackson and Yielding, 1983; Prevot et al., 1980; Seeber and Armbruster, 1979].

In addition to the abundant shallow earthquake activity bounding the basin, intermediate-depth seismicity occurs in a south dipping zone beneath the Pamir and in a north dipping zone beneath the Hindu Kush (Figure 2). The south dipping seismic zone extends from about 100 km to 250 km depth and projects through a "quiet zone" to the surface near the Darvaz-Karakul fault at the southern edge of the Peter I range [e.g., Chatelain et al., 1980; Billington et al., 1977]. The north dipping seismic zone extends from 70 to 250 km depth and projects to the surface between the Panjer and Kunar faults south of the Hindu Kush [e.g., Chatelain et al., 1980; Roecker et al., 1980; Billington et al., 1977]. Roecker [1982] found low seismic velocities associated with the north dipping zone and inferred that continental crust is being subducted beneath the Hindu Kush. Abundant shallow earthquakes in the Peter I range give evidence that the south dipping seismic zone is contiguous with surface deformation here. However, diffuse shallow seismicity in the Hindu Kush is not obviously linked to the north dipping zone and indicates that subduction here has a complex surface expression.

BODY WAVE INVERSION FOR SOURCE MECHANISMS

Method

A waveform-fitting inversion technique was used to obtain reliable focal mechanisms and depths for the earthquakes [e.g., McCaffrey and Nábělek, 1987; Nábělek, 1984] from analog seismograms recorded by the World-Wide Standard Seismograph Network (WWSSN). Long-period P waves were used from stations at epicentral distances between 30° and 90° and SH waves at distances from 30° to 70°. P and SH phases were hand-digitized, interpolated at 0.5 s intervals, and detrended. The two earthquakes presented

here were the only shallow events near the northern Hindu Kush recorded by the WWSSN that were large enough to be studied with this method.

The earthquake source was parameterized by source depth, moment, source-time function, and double-couple orientation specified by the strike, dip, and rake of one nodal plane, using the convention of Aki and Richards [1980]. Source parameters were estimated by minimizing the difference between the observed and calculated seismograms (the Variance in Table 2) in a least squares sense. Arrival times for the direct phases were adjusted by cross correlation between observed and calculated seismograms but were not allowed to change by more than 1.0 s if impulsive first arrivals were visible.

Because standard errors determined from the least squares inversion can grossly misrepresent the true uncertainties of the solution, a series of experiments served to estimate acceptable ranges of values for source parameters (Figures 3,5,6,8,9 and Table 2). In each test the value of the parameter being studied was held fixed while all of the other parameters were determined by inversion. The effects of varying the assumed sedimentary layer thickness in the source region were investigated in a similar fashion. Uncertainties were estimated from the resulting waveforms by visually inspecting the match between calculated and observed seismograms. Similar calculations were conducted by McCaffrey and Nábělek [1987] and Nelson et al. [1987] to determine uncertainties for other source parameters for large thrust earthquakes.

Source Structure

Reflections from sediment-basement interfaces are often seen in seismograms from earthquakes under deep basins and can affect the determination of both depth and source time function [e.g., Huang et al., 1986]. Sometimes, subsurface reflections can be used to constrain sediment thickness near the earthquakes [e.g., McCaffrey and Nábělek, 1987; Nelson et al., 1987]. Southern Tadjik basin sediments reach a maximum thickness of 10-12 km within 50 km of the reported epicenters of both earthquakes [Marussi, 1963; Zakharov et al., 1968] and appear to produce reflections noticeable on some seismograms. Therefore the source region

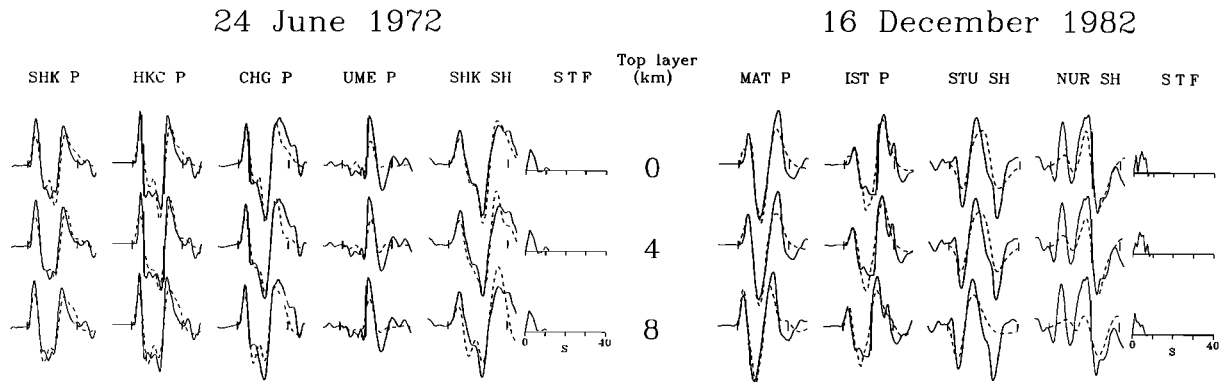


Fig. 3. Observed (solid) and calculated (dashed) seismograms for different thicknesses of the sedimentary layer. Top line labels the earthquake, next line labels the station and phase for each seismogram. Seismograms are scaled to the seismic moment calculated for each earthquake, corrected to a common magnification and geometrical spreading factor. SH amplitudes are reduced 2/3 relative to P amplitudes. "S.T.F." is the source-time function calculated for each earthquake and for each sedimentary thickness, with horizontal scale bar in seconds.

was parameterized by a thin layer representing basin sediments over a half-space. The sedimentary layer had P and S velocities fixed to 3.5 and 2.0 km/s, respectively, and a density of 2000 kg/m³. The half-space had crustal P and S velocities of 6.5 and 3.7 km/s, respectively, and a density of 2900 kg/m³. The thickness of the layer of sediments varied from 0 to 8 km in different tests aimed at evaluating the uncertainties in the source parameters and velocity structure.

The match between calculated and observed seismograms (Figure 3 and Table 2) does not vary in a simple way with sediment thickness but depends on the station azimuth, the phase, and the earthquake. For the 1972 event, P waves recorded by stations to the east (SHK P, HKC P, and CHG P on Figure 3) show arrivals between the direct P and phases reflected from the free surface (pP and sP) that can be matched if 4 km of sediments are placed over the source. Stations west of the 1972 earthquake (e.g., UME P on Figure 3) recorded a nearly nodal direct-P arrival and should have clear arrivals from upgoing phases reflected off the base of the sediments; these stations are best matched with an 8-km-thick sedimentary layer. P waves from the 1982 event are relatively insensitive to sediment thickness, except that when a sediment-free half-space is used, the first half cycle becomes too broad,

resulting in alignment errors. SH waveforms for both earthquakes are matched using either a half-space or 4 km of sediments over a half-space. Thus reflections due to near-source structure are probably contributing to the observed waveforms, but the identification of specific arrivals is ambiguous. A 4-km-thick layer was used in all the other calculations presented here, but nearly identical source parameters were estimated when a half-space structure was assumed.

JUNE 24, 1972

This earthquake ($m_b=6.0$) caused some damage and fatalities near Ishkamish, Afghanistan on the northern flank of the Hindu Kush (Figure 2) and was located by the International Seismological Centre (ISC) at 47 km depth. We determined a nearly pure thrust mechanism showing northwest-southeast compression at 24 km depth, with a moment of 2×10^{18} N-m and a duration of 6.6 s (Figure 4 and Table 1). P waves show small or nearly nodal direct arrivals at stations to the northwest, but impulsive arrivals at stations to the southeast, indicating that one nodal plane dips steeply to the northwest. Compressional arrivals at KBS and AAE, together with many nodal and dilatational arrivals at European stations, constrain the dip to within 10° of the preferred value.

24 June 1972

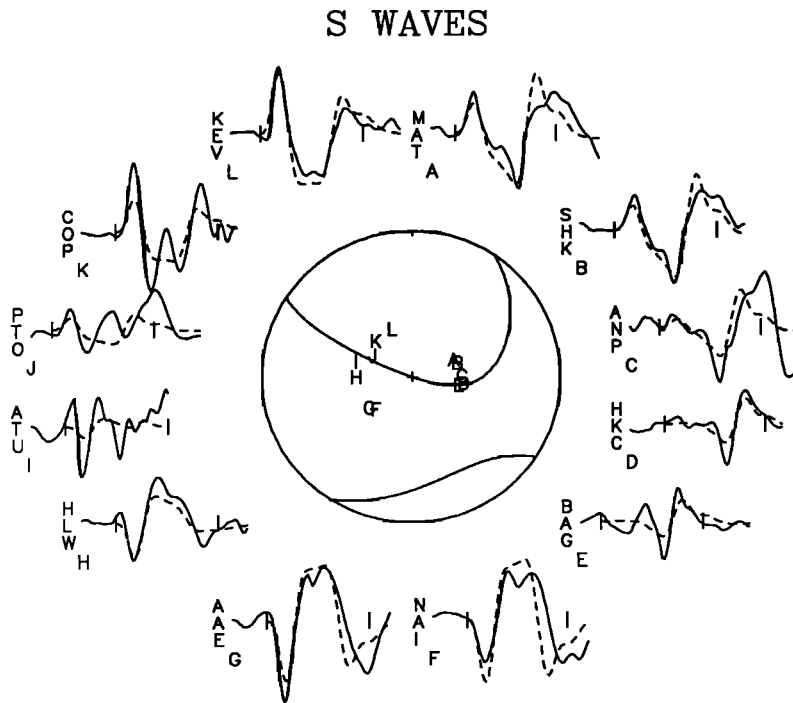
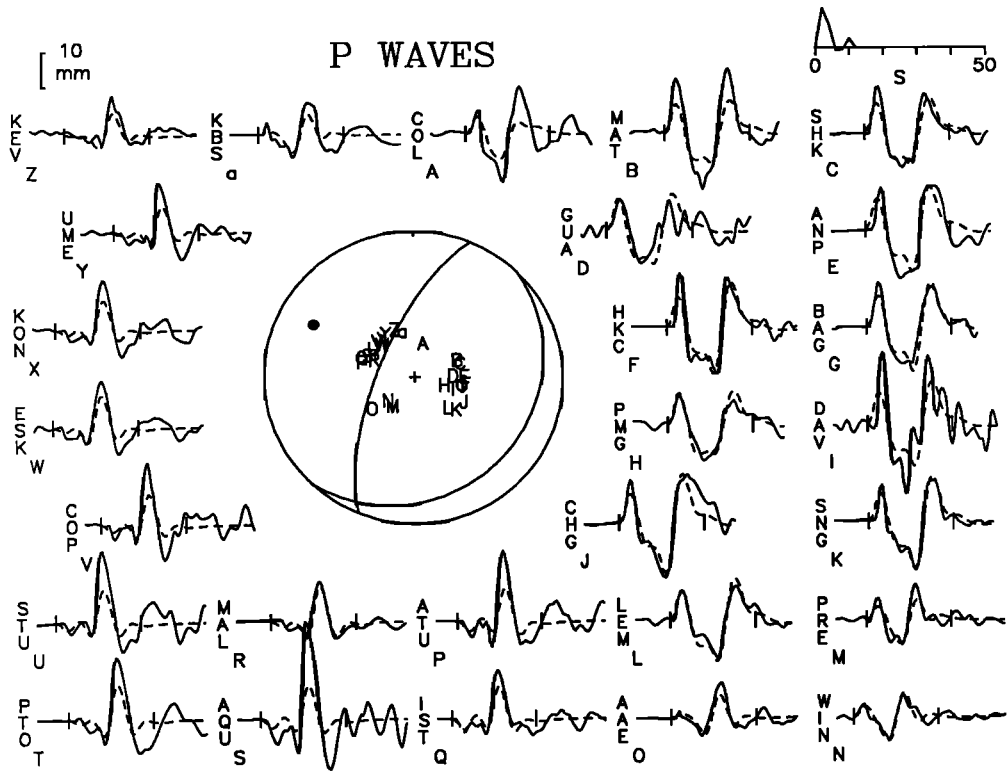


TABLE 1. Earthquake Source Parameters, With Formal Uncertainties (1- σ)

	June 24, 1972	December 16, 1982
Origin Time ^a	1529:22.3	0040:48.6
Latitude ^a	36.28°N	36.13°N
Longitude ^a	69.69°E	68.98°E
m_b (NEIS)	6.0	6.2
Number of stations ^a	336	530
Depth, km	24.0 \pm 0.7	22.0 \pm 0.8
M_0 , 10 ¹⁸ Nm	1.85 \pm 0.69	5.54 \pm 6.39
Duration ^b , s	6.6	7.2
Nodal plane 1:		
Strike, deg	203 \pm 2	225 \pm 2
Dip, deg	70 \pm 1	48 \pm 0
rake, deg	83 \pm 4	100 \pm 1
Nodal plane 2:		
Strike, deg	44	30
Dip, deg	21	43
P axis:		
Azimuth, deg	298	308
Plunge, deg	25	3
T axis:		
Azimuth, deg	100	198
Plunge, deg	64	82
Number of waveforms used:		
P	27	19
S	12	10

^aFrom ISC (International Seismological Centre, Edinburgh) catalog.

^bDuration = 2 x (centroid time - origin time), from source-time function.

The estimated strike of the northwest dipping nodal plane is 203°. Because the direction of shortening implied by the mechanism found from waveform inversion (298°) differs substantially from that predicted by major-plate motions (337° [Minster and Jordan, 1978]), we present tests used to determine the uncertainty in the estimated strike (Figure 5). P wave polarities (e.g., KEV P) at the nearly nodal European stations are violated as the strike angle decreases 15° as are the polarities of East Asian SH records (HKC

SH). Because inferences of strike and dip are not independent (Table 2), the European P waves allow a more east-west strike, but the polarities of some European SH records (COP SH) and amplitudes of some reflected phases (CHG P) are not matched. Thus we estimate the uncertainty in strike (and hence the slip direction on the southeast dipping plane) to be 15° or less.

Tests that fix the hypocenter at various depths show that the depth of the event appears to be within 5 km of 24 km

Fig. 4. Preferred solution for the 1972 earthquake with all seismograms used in analysis. P waves are shown on top and SH waves are on the bottom, with the nodes of the corresponding radiation patterns. Small solid and open circles on the P wave focal sphere designate the P and T axes, respectively. Solid lines are observed seismograms, dashed lines are calculated. The source-time function and horizontal scale bar are shown in the top right corner, and the vertical scale bar is in the top left corner. Seismogram amplitudes are corrected to a magnification of 3000 and a distance of 40°. The amplitude scale for the seismograms is in the top left corner. Small letters on the focal spheres show positions of rays to stations and correspond to letters next to the waveforms below the station names.

24 June 1972

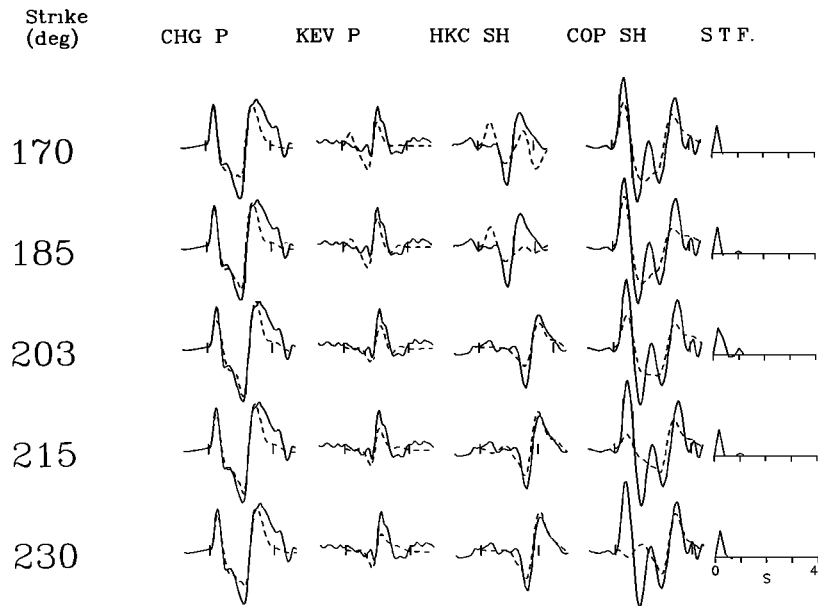


Fig. 5. Observed and calculated seismograms for four stations for different strikes of the 1972 earthquake. Format is same as for Figure 3.

(Figure 6). At depths of 30 km or more the calculated depth phases arrive too late at all stations (even when the source region is a sediment-free half-space). The amplitudes and shapes of most observed waveforms are not matched at 10 and 15 km depth, and at 20 km depth the observed relative timing of direct and reflected SH phases (first and second peaks of SHK SH) is not matched. The depth is somewhat dependent on the thickness of the low-velocity layer above it (see "Sedimentary Layer" test in Table 2), because the average vertical slowness above the source increases with increasing layer thickness and because near-surface reflections are partly coupled to the source time function. For example, with 8 km of sediments the earthquake was located at 17.5 km depth. Considering all these uncertainties, the source depth is constrained to be between 15 and 30 km, which implies that the hypocenter is well below the sediments. Possibly, the fault ruptured into the basin.

DECEMBER 16, 1982

This earthquake is the largest shallow event in the southern Tadjik basin region ($m_b=6.2$; $m_s=6.7$) since the WSSN was

installed. It resulted in over 500 deaths and extensive damage in the Baghlan province of Afghanistan. The seismic moment was determined to be 6×10^{18} N m, 3 times that of the 1972 event, although the source duration appears to be nearly the same (Table 1). The inferred mechanism (Figure 7) reveals almost pure thrust faulting at 22 km depth (compared with 35 km determined by the ISC). The azimuth of the P axis is similar to that of the 1972 event, but the dips of the nodal planes are different, in that impulsive direct-P arrivals at all azimuths constrain the dip of both nodal planes to be within 10° - 15° of 45° . We examined the effects of rupture propagation due to a finite source to determine which plane was the fault plane but were unable to document any significant effects.

Detailed tests of the strike and depth uncertainties were made. The P waves are nearly identical at all azimuths and do not constrain the strike. SH wave polarities, however, show a node in the SH radiation pattern that falls between stations STU and NUR, suggesting a 15° uncertainty in the strike (Figure 8). P waves for seismograms calculated at depths between 15 and 25 km (Figure 9) fit the

TABLE 2a. Determination of Uncertainties, June 24, 1972.

Sediment Thickness	Depth, km	Mo, 10^{18} N m	Duration, s	N.P.1:			N.P.2:			P axis:		T axis:		Variance ^a
				Strike	Dip	Rake	Strike	Dip	Azi-	Plunge	Azi-	Plunge		
Sedimentary Thickness Test														
0 km	25.1	1.77	6.2	203	72	84	43	20	298	26	103	63	1.1039	
4 km	24.0	1.85	6.6	203	70	83	44	21	298	25	100	64	1.0000	
8 km	17.5	2.23	7.0	203	66	83	40	25	298	21	100	68	1.0132	
Depth Test														
4 km	10.0	2.91	11.0	201	70	83	40	21	296	25	100	64	1.6770	
4 km	15.0	2.64	9.2	201	59	92	18	31	290	14	116	76	1.3311	
4 km	20.0	1.63	8.6	201	67	88	25	23	292	22	108	67	1.1688	
4 km	24.0	1.85	6.6	203	70	83	44	21	298	25	100	64	1.0000	
4 km	30.0	1.39	3.8	216	66	75	70	28	318	20	100	66	1.5654	
4 km	35.0	1.34	3.6	237	61	69	96	35	342	14	107	66	2.0399	
Strike Test														
4 km	24.5	1.63	3.8	170	65	115	303	34	242	17	118	62	1.3459	
4 km	23.8	1.75	5.2	185	68	106	328	27	263	21	121	64	1.1160	
4 km	24.0	1.85	6.6	203	70	83	44	21	298	25	100	64	1.0000	
4 km	24.2	1.79	5.4	215	67	72	76	29	319	20	95	63	1.0917	
4 km	24.6	1.76	4.8	230	63	63	98	37	339	14	98	62	1.2428	

^amean-squared residual between observed and calculated seismograms; normalized to best solution.

TABLE 2b. Determination of Uncertainties, December 16, 1982.

Sediment Thickness	Depth, km	Mo, 10^{18} N m	Duration, s	N.P.1:			N.P.2:			P axis:		T axis:		Variance ^a
				Strike	Dip	Rake	Strike	Dip	Azi-	Plunge	Azi-	Plunge		
Sedimentary Thickness Test														
0 km	22.8	5.45	7.0	225	48	101	30	43	308	3	198	82	0.9977	
4 km	22.0	5.54	7.2	225	48	100	30	43	308	3	198	82	1.0000	
8 km	17.5	5.84	5.0	231	49	96	42	42	317	3	191	84	1.3754	
Depth Test														
4 km	10.0	5.52	7.0	232	50	95	44	40	318	5	177	83	1.7393	
4 km	15.0	5.78	5.8	232	49	98	39	41	316	4	195	83	1.3784	
4 km	20.0	5.59	8.2	226	48	100	30	43	308	3	199	82	1.1105	
4 km	22.0	5.54	7.2	225	48	100	30	43	308	3	198	82	1.0000	
4 km	25.0	5.29	5.4	226	48	100	31	43	309	3	199	82	1.0677	
4 km	30.0	4.23	2.8	232	48	102	35	43	314	3	207	81	1.6414	
Strike Test														
4 km	22.6	5.34	6.6	195	46	101	359	45	277	1	183	82	1.6414	
4 km	22.2	5.40	7.2	210	47	101	14	44	292	2	191	82	1.2273	
4 km	22.0	5.54	7.2	225	48	100	30	43	308	3	198	82	1.0000	
4 km	21.2	5.32	7.6	240	49	100	44	42	323	4	208	81	1.1556	
4 km	21.2	4.34	8.2	255	51	100	60	40	338	5	214	81	1.6258	

^amean-squared residual between observed and calculated seismograms; normalized to best solution.

24 June 1972

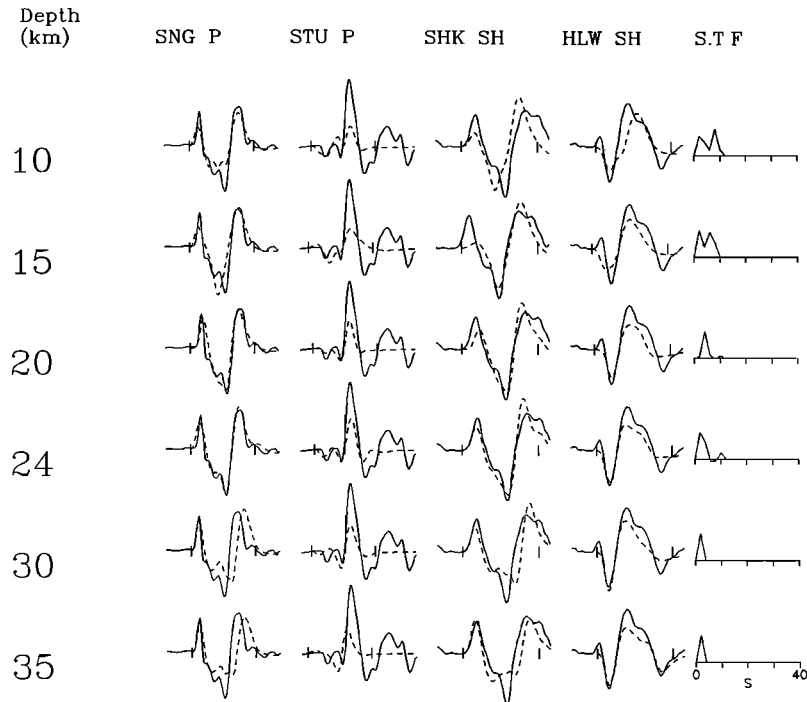


Fig. 6. Observed and calculated seismograms for four stations for different depths of the 1972 earthquake. Format is same as for Figure 3.

waveforms reasonably well (SLR and IST), but the observed SH seismograms are only matched at 20, 22, and 25 km (STU and KEV). Thus the estimated 22-km depth for this event has an uncertainty of approximately 5 km when a 4-km-thick sedimentary layer is assumed, increasing to 7-8 km when the uncertainty in source structure is taken into account.

In order to place further constraints on faulting, aftershocks for the 1982 earthquake were relocated. We used a master-event method, setting arrival-time residuals for the main event as station corrections for the aftershocks. Most of the aftershocks cluster 10-15 km northeast of the main shock, with one 35 km to the northeast. Reliable depths for the aftershocks could not be determined, probably because there were no stations within 150 km of the events. Without reliable depths the aftershock distribution does not define uniquely a fault plane orientation, although it is parallel to the nodal planes of the focal mechanism.

DISCUSSION

Both earthquakes show thrust faulting, with small strike-slip components. The P axes of both mechanisms are not parallel to the direction of India-Eurasia convergence, but the fault planes strike parallel to local structures. The mechanisms suggest that the Tadjik basin is not behaving as an independent rigid block that is being displaced westward along strike-slip faults. Rather, the Hindu Kush is advancing northward toward the Tien Shan and overriding the intervening Tadjik basin. The discrepancy between the direction of maximum shortening for the earthquakes (the P axes) and the direction of large-scale convergence may be explained if the Pamirs are overthrusting to the west as well as advancing to the north. Paleomagnetic observations also suggest that the Pamirs are advancing westward over the Tadjik basin, by counterclockwise rotation of the western Pamirs relative to Eurasia and the central Pamirs [e.g., Bazhenov and Burtman, 1986].

16 December 1982

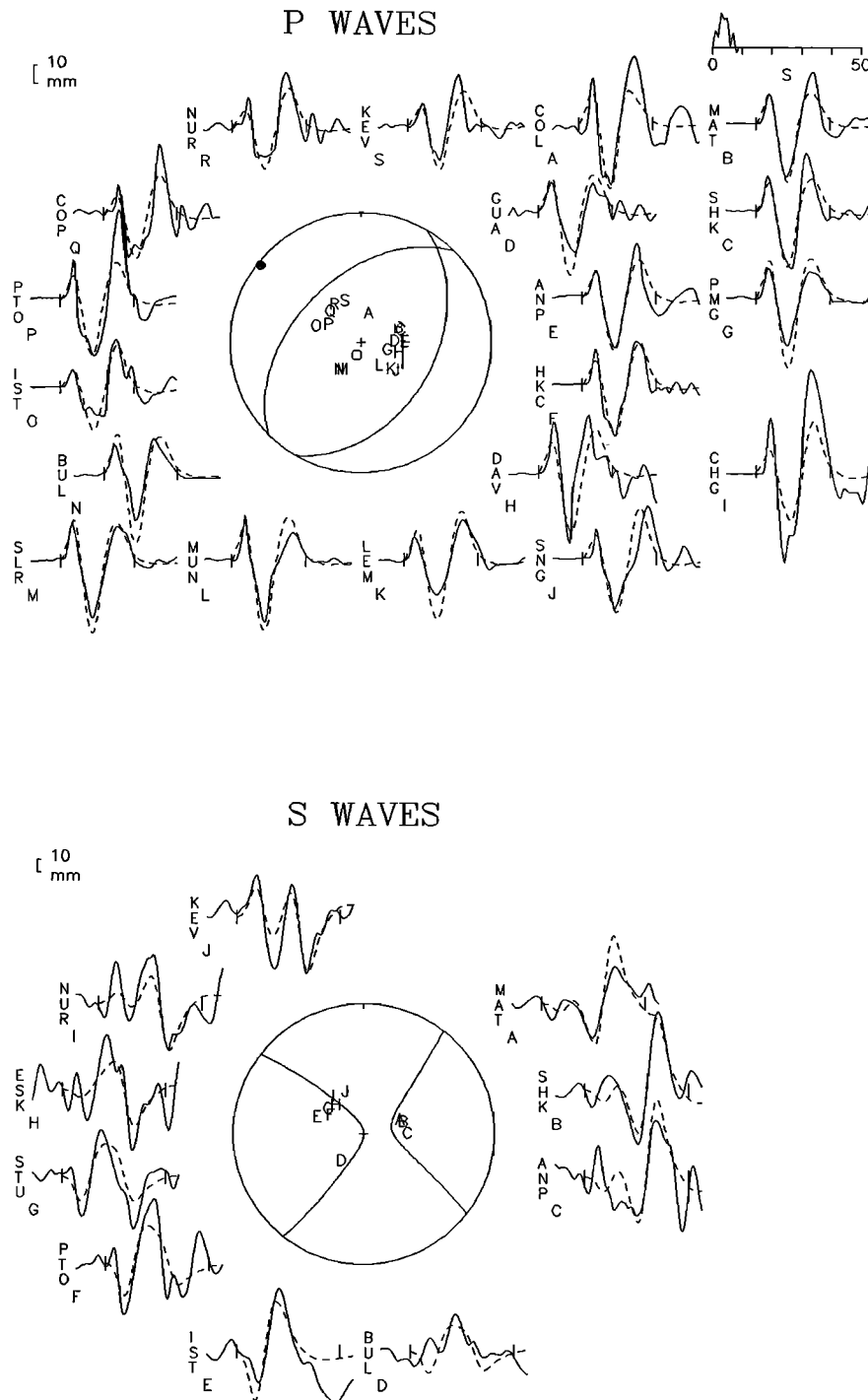


Fig. 7. Preferred solution for 1982 earthquake, with all observed and calculated seismograms used in the least squares determination. Format is same as for Figure 4, except P and SH waveforms have different vertical scales.

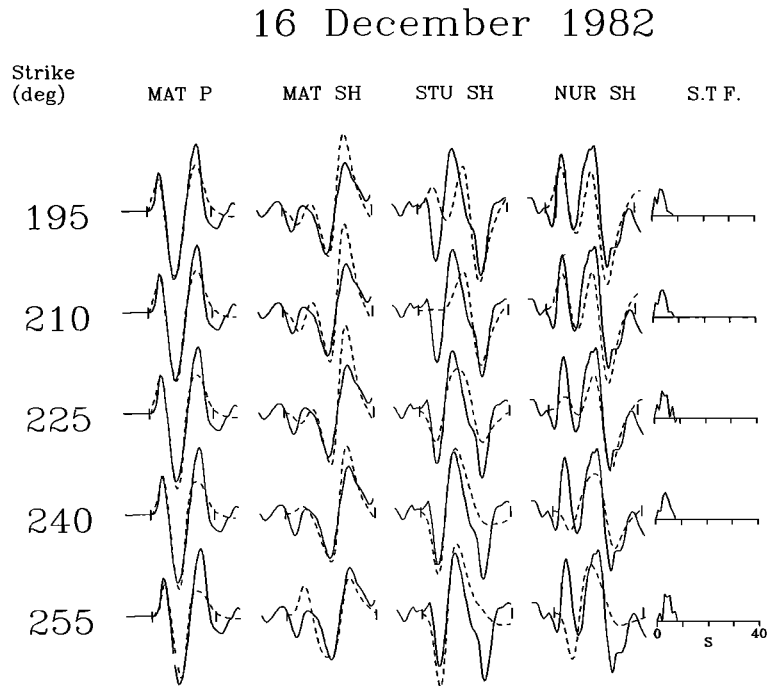


Fig. 8. Observed and calculated seismograms for four stations for different strikes of the 1982 earthquake. Format is same as for Figure 3.

Thrust belt structures in the Tadjik basin, as well as the relative topography and gravity of the Hindu Kush and the basin, suggest that the fault planes for the earthquakes are represented by the southeast dipping nodal planes. Large accumulations of east dipping Plio-Pleistocene molasse are found in the eastern Tadjik basin near the events [Tapponnier et al., 1981], and foreland thrust belt structures are documented to the north [Leith and Alvarez, 1985]. The Hindu Kush range is 3-5 km higher in elevation than the basin (Figures 1 and 10a) and a 40-50 mGal isostatic gravity low is associated with the basin [Marussi, 1963]. Thus, it is more plausible that the mountains are overriding the basin rather than the reverse and that the southeast dipping nodal planes are the fault planes.

Estimated depths place the earthquakes well into the basement below the basin sediments. Along with the fairly steep dips on the nodal planes, these depths imply that the events are occurring neither within shallow thrust sheets nor along horizontal detachment surfaces.

Several explanations can be made to relate inferred basement faulting to detachment structures in the sediments. One possibility is that the basement faults continue steeply to the surface at the edge of the Hindu Kush, carrying the Hindu Kush basement directly over the basin. However, the 1982 earthquake was located 10-15 km northwest of the exposed pre-Mesozoic basement, so in order for this fault geometry to be viable the earthquake must be significantly mislocated, or other buried basement faults must exist. An alternative mechanism, proposed by Jackson [1980], is that distributed high-angle faults may accommodate basement shortening below fold belts of detached sediments such as the Zagros. Such a fault geometry may exist in the Tadjik basin (Figure 10b); however, the proximity of almost all the large ($m_b > 5$) earthquakes to the southeastern edge of the basin (Figure 2) suggests that basement shortening is more localized.

Basement faulting may be directly connected to the shallow thrust faults observed in the basin sediments farther northwest (Figure 10c). Shallow

16 December 1982

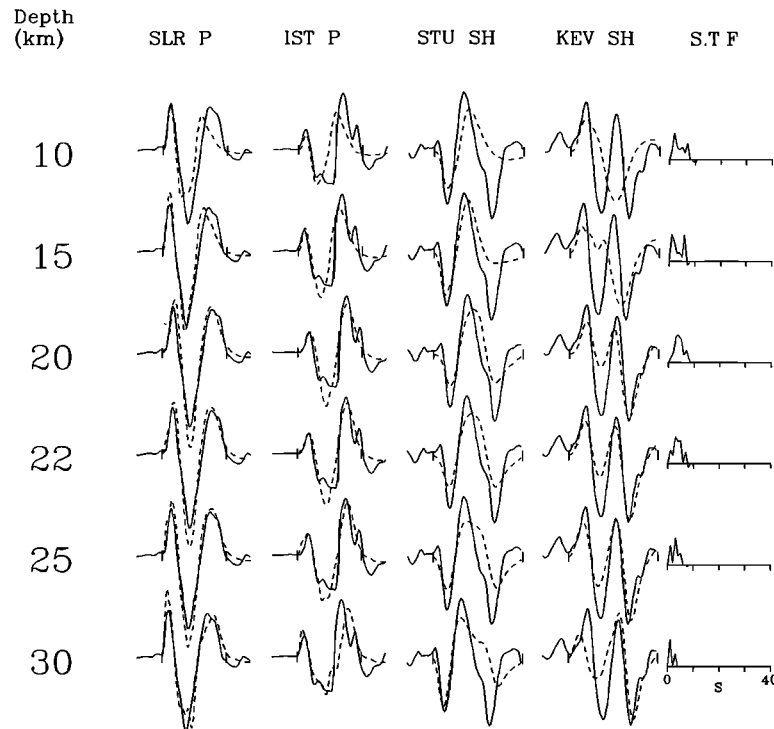


Fig. 9. Observed and calculated seismograms for four stations for different depths of the 1982 earthquake. Format is same as for Figure 3.

detachment faults may be nearly horizontal along weak sedimentary layers such as within the Jurassic evaporites and steepen into the underlying basement near the eastern edge of the basin. Similar high-angle faulting at midcrustal depths in the Peruvian sub-Andes has been shown to be related to shallow faulting in sediments on the Brazilian shield [Suárez et al., 1983].

The Peter I range north of the Pamirs is composed of highly deformed basin sediments similar to those found in the Tadjik basin and may record the nearly complete closing of an eastward extension of the basin. The lithosphere originally beneath these sediments is found to 150 km depth beneath the Pamirs in a south dipping seismic zone. The presence of active thrusting at the southern margin of the Tadjik basin indicates that the slightly deformed Tadjik basin is closing and eventually may be reduced to a western extension of the Peter I range. This will require up to 200 km of shortening in the

Tadjik basin basement, either through subduction or crustal thickening.

Many more shallow earthquakes are found north of the Hindu Kush, in the Tadjik basin, than immediately to the south of the mountains (Figures 2, 10d) even though the north dipping seismic zone projects to the surface south of the ranges near the Kunar fault [Chatelain et al., 1980]. This may indicate that north dipping subduction of continental lithosphere is encountering resistance and that a substantial amount of crustal convergence is presently being accommodated north of the Hindu Kush.

The position of the southeast dipping thrusts north of the Hindu Kush relative to the deep seismic zone (Figure 10d) suggests an analogy to back arc thrusting behind oceanic island arcs, observed (for example) behind Japan [Fukao and Furumoto, 1975], the eastern Sunda arc [Silver et al., 1983], and, in particular, north of the Timor trough [McCaffrey and Nábelek, 1986]. Near Timor, no subduction

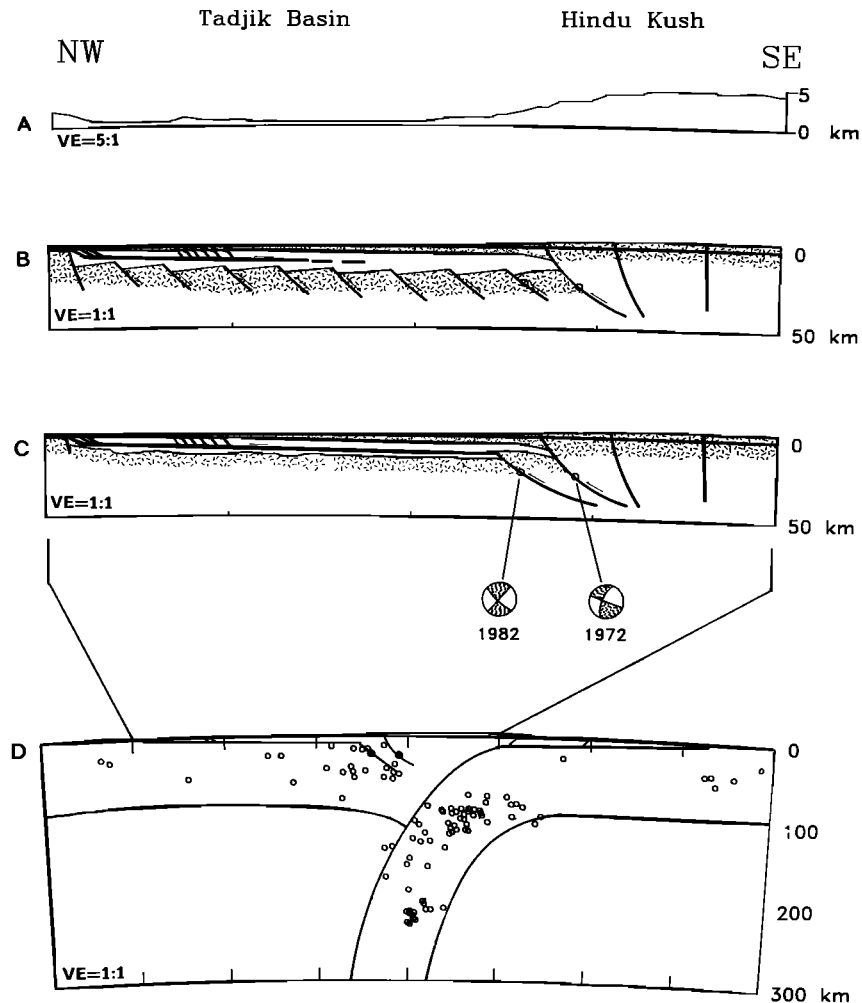


Fig. 10. Cartoons illustrating hypothetical structures in the Tadjik basin. Near-surface geology is based on descriptions by Shareq [1981], Tapponnier et al. [1981] and Leith and Alvarez [1985]; upper-mantle structure is based on interpretations by Tapponnier et al. [1981] and observations by Roecker [1982]. All cross sections follow great circle arcs oriented NW-SE, and A-C are centered at 37°N, 69°E. Horizontal tic marks are at 1° intervals, and "VE" refers to vertical exaggeration. (a) Topography for profiles B and C. Values are averaged at 10 km intervals along the profile, from a global set of 5-min elevation averages (DBDB5). (b) Cartoon showing basement shortening taken up along distributed thrust faults below a detachment surface, following Jackson's [1980] explanation for basement thrust faulting in the Zagros. Thrust faults are hypothesized to be reactivated normal faults, originally associated with rifting. Locations are shown for the earthquakes studied here (open circles). Heavy lines are faults and light lines are contacts. Randomly oriented line segments indicate crystalline basement, stippled region represents Neogene molasse, and unshaded region in basin represents marine sediments. (c) Cartoon showing basement shortening concentrated in the southeast along high-angle thrust faults which are downdip extensions of detachment thrusts in the sediments. Focal mechanisms for the events studied are shown as back-hemisphere projections. (d) Deep structure and seismicity below the Hindu Kush-Tadjik Basin region, showing seismicity and the apparent relationship between shallow thrusting and deeper subduction. Criteria for selecting earthquakes are the same as for events plotted in Figure 2. The earthquakes analyzed in this study are shown as solid circles, and other earthquakes are shown as open circles.

earthquakes have been documented where the Australian continent has collided with the island arc, but large thrust earthquakes are found north of the arc [e.g., McCaffrey et al., 1985; McCaffrey and Nábělek, 1986]. Buoyant continental crust appears to have been subducted to substantial depths beneath both Timor and the Hindu Kush [McCaffrey et al., 1985; Roecker, 1982], making continued subduction more difficult than thrusting behind the "arc". In both examples it is difficult to know whether the back arc thrusting will develop into a new subduction zone (i.e., an arc-polarity reversal), the existing subduction will be maintained, or convergence will be taken up by some other mechanism such as crustal thickening. In any case, the presence of large thrust earthquakes behind the "arc" implies that there is substantial coupling between the plates and that subduction alone is insufficient to accommodate convergence.

Acknowledgments. This manuscript was improved by comments and suggestions by P. Molnar, B.C. Burchfiel, L. Seeber, and two anonymous reviewers. C. Bryan and G. Abers both acknowledge support from NSF Graduate Fellowships. Publication costs were partially funded by NSF contracts EAR-8618384 and EAR-8608405.

REFERENCES

- Aki, K., and P. G. Richards, Quantitative Seismology, Theory and Methods, 557 pp., W. H. Freeman, San Francisco, Calif., 1980.
- Baranowski, J., J. Armbruster, L. Seeber, and P. Molnar, Focal depths and fault plane solutions of earthquakes and active tectonics of the Himalaya, J. Geophys. Res., **89**, 6918-6928, 1984.
- Bazhenov, M. L., and V. S. Burtman, Tectonics and paleomagnetism of structural arcs of the Pamir-Punjab Syntaxis, J. Geodyn., **5**, 383-396, 1986.
- Billington, S., B. L. Isacks, and M. Barazangi, Spatial distribution and focal mechanisms of mantle earthquakes in the Hindu-Kush-Pamir region: A contorted Benioff zone, Geology, **5**, 699-704, 1977.
- Chatelain, J. L., S. W. Roecker, D. Hatzfeld, and P. Molnar, Microearthquake seismicity and fault plane solutions in the Hindu Kush region and their tectonic implications, J. Geophys. Res., **85**, 1365-1387, 1980.
- England, P., and G. Houseman, Role of lithospheric strength heterogeneities in the tectonics of Tibet and neighboring regions, Nature, **315**, 297-301, 1985.
- Fukao, Y., and M. Furumoto, Mechanism of large earthquakes along the eastern margin of the Japan sea, Tectonophysics, **25**, 247-266, 1975.
- Gubin, I. Y., Patterns of Seismic Activity in Tadjikistan (in Russian), 450 pp., Academy of Sciences of the USSR, Moscow, 1960.
- Hatzfeld, D., S. W. Roecker, J. Nábělek, and B. Tucker, Seismicity in the Garm region of Central Asia: Deformation in a zone of continental convergence, Ann. Geophys. Gauthier Villars, **4**, 555-566, 1986.
- Huang, P. Y., S. C. Solomon, E. A. Bergman, and J. L. Nábělek, Focal depths and mechanisms of Mid-Atlantic Ridge earthquakes from body waveform inversion, J. Geophys. Res., **91**, 579-598, 1986.
- Jackson, J., and G. Yielding, The seismicity of Kohistan, Pakistan: Source studies of the Hamran (1972.9.3), Darel (1981.9.12) and Patan (1974.12.28) earthquakes, Tectonophysics, **91**, 15-28, 1983.
- Jackson, J. A., Reactivation of basement faults and crustal shortening in orogenic belts, Nature, **283**, 343-346, 1980.
- Kuchai, V. K., and V. G. Trifonov, Young sinistral shearing along the Darvaz-Karakul fault zone, Geotectonics, **11**, 218-226, 1977.
- Leith, W., Rock assemblages in Central Asia and the evolution of the Southern Asian margin, Tectonics, **1**, 303-318, 1982.
- Leith, W., and W. Alvarez, Structure of the Vakhsh fold-and-thrust belt, Tadjik SSR: Geologic mapping on a Landsat image base, Geol. Soc. Am. Bull., **96**, 875-885, 1985.
- Marussi, A., Le anomalie della gravita lungo la catena del Karakorum-Hindu Kush, publication, pp. 198-210, Ist. di Geod. e Geofis., Rome, 1963.
- McCaffrey, R., and J. Nábělek, Seismological evidence for shallow thrusting north of the Timor trough, Geophys. J. R. Astron. Soc., **85**, 365-381, 1986.
- McCaffrey, R., and J. Nábělek, Earthquakes, gravity, and the origin of the Bali basin: An example of a nascent continental fold-and-thrust belt, J. Geophys. Res., **92**, 441-460, 1987.

- McCaffrey, R., P. Molnar, S. W. Roecker, and Y. S. Joyodiwiryo, Microearthquake seismicity and fault plane solutions related to arc-continent collision in the eastern Sunda arc, Indonesia, *J. Geophys. Res.*, **90**, 4511-4528, 1985.
- Minster, J. B., and T. H. Jordan, Present-day plate motions, *J. Geophys. Res.*, **83**, 5331-5354, 1978.
- Molnar, P., and Q. Deng, Faulting associated with large earthquakes and the average rate of deformation in central and eastern Asia, *J. Geophys. Res.*, **89**, 6203-6227, 1984.
- Molnar, P., and P. Tapponnier, Cenozoic tectonics of Asia: Effects of a continental collision, *Science*, **189**, 419-426, 1975.
- Nábělek, J. L., Determination of earthquake source parameters from inversion of body waves, Ph.D. thesis, 262 pp., Mass. Inst. of Technol., Cambridge, 1984.
- Nelson, M. R., R. McCaffrey, and P. Molnar, Source parameters for 11 earthquakes in the Tien Shan, central Asia, determined by P and SH waveform inversion, *J. Geophys. Res.*, **92**, 12,629-12,648, 1987.
- Peive, A. V., V. S. Burtman, S. V. Ruzhentsev, and A. I. Suvorov, Tectonics of the Pamir-Himalayan sector of Asia, *Rep. Sess., Int. Geol. Congr.*, **22**, 441-464, 1964.
- Prevot, R., D. Hatzfeld, S. W. Roecker, and P. Molnar, Shallow earthquakes and active tectonics in eastern Afghanistan, *J. Geophys. Res.*, **85**, 1347-1357, 1980.
- Roecker, S. W., Velocity structure of the Pamir-Hindu Kush region: Possible evidence of subducted crust, *J. Geophys. Res.*, **87**, 945-959, 1982.
- Roecker, S. W., O. V. Soboleva, I. L. Nersesov, A. A. Lukk, D. Hatzfeld, J. L. Chatelain, and P. Molnar, Seismicity and fault plane solutions of intermediate depth earthquakes in the Pamir-Hindu Kush region, *J. Geophys. Res.*, **85**, 1358-1364, 1980.
- Seeber, L., and J. Armbruster, Seismicity of the Hazara arc in northern Pakistan: Decollement vs. basement faulting, in *Geodynamics of Pakistan*, edited by A. Farah and K. A. DeJong, Geological Survey of Pakistan, Quetta, 131-142, 1979.
- Shareq, A., Tectonic map of Afghanistan, in *Zagros, Hindu Kush, Himalaya: Geodynamic Evolution*, *Geodyn. Ser.*, vol. 3, edited by H. K. Gupta and F. M. Delany, Map 1, AGU, Washington, D. C., 1981.
- Silver, E. A., D. R. Reed, R. McCaffrey, and Y. S. Joyodiwiryo, Backarc thrusting in the eastern Sunda arc, Indonesia: A consequence of arc-continent collision, *J. Geophys. Res.*, **88**, 7429-7448, 1983.
- Stöcklin, J., Structural correlation of the Alpine ranges between Iran and Central Asia, in *Livre a la Memoire de Albert F. de Lapparent*, pp. 333-353, Société Géologique de France, Paris, 1977.
- Suárez, G., P. Molnar, and B. C. Burchfiel, Seismicity, fault plane solutions, depth of faulting, and active tectonics of the Andes of Peru, Ecuador, and southern Colombia, *J. Geophys. Res.*, **88**, 10,403-10,428, 1983.
- Tapponnier, P., M. Mattauer, F. Proust, and C. Cassaigneau, Mesozoic ophiolites, sutures, and large-scale tectonic movements in Afghanistan, *Earth Planet. Sci. Lett.*, **52**, 355-371, 1981.
- Tapponnier, P., G. Peltzer, A. Y. LeDain, R. Armijo, and P. Cobbold, Propagating extrusion tectonics in Asia: New insights from simple experiments with plasticene, *Geology*, **10**, 611-616, 1982.
- Trifonov, V. G., Late Quaternary tectonic movements of western and central Asia, *Geol. Soc. Am. Bull.*, **89**, 1059-1072, 1978.
- Wellman, H. N., Active wrench faults of Iran, Afghanistan, and Pakistan, *Geol. Rundsch.*, **55**, 716-735, 1966.
- Wesson, R. L., V. G. Leonova, A. B. Maximov, I. L. Nersesov, and F. G. Fischer, Results of a common field seismological investigation in the Peter I Range area in 1975, in *The Soviet-American Exchange in Earthquake Prediction* (in Russian), 1, pp. 43-69, Donish, Dushanbe, USSR, 1976.
- Zakharov, S. A., M. M. Kukhtikov, Y. Y. Leven, and G. T. Vinnichenko, Tectonics, in *Atlas of Tadjikistan* (in Russian), edited by A. P. Nebzevetskii, pp. 17-20, Academy of Sciences of Tadjikistan, Dushanbe, USSR, 1968.

G. Abers, C. Bryan, and R. McCaffrey, Department of Earth, Atmospheric and Planetary Sciences, Massachusetts Institute of Technology, Cambridge MA 02139.

S. Roecker, Department of Geology, Rensselaer Polytechnic Institute, Troy NY 12180.

(Received May 29, 1987;
revised October 20, 1987;
accepted October 20, 1987.)